


Cite this: *RSC Adv.*, 2020, 10, 10826

# Synthesis and application of coumarin fluorescence probes

Xiao-ya Sun,<sup>acd</sup> Teng Liu,<sup>bcd</sup> Jie Sun<sup>id</sup>\*<sup>bcd</sup> and Xiao-jing Wang\*<sup>bcd</sup>

In recent years, the research on fluorescent probes has developed rapidly. Coumarin fluorescent probes have also been one of the hot topics in recent years. For the synthesis and application of coumarin fluorescent probes, great progress has been made. Coumarin fluorescent probes have become more and more widely used in biochemistry, environmental protection, and disease prevention, and have broad prospects. This review introduces the three main light emitting mechanisms (PET, ICT, FRET) of fluorescent probes, and enumerates some probes based on this light emitting mechanism. In terms of the synthesis of coumarin fluorescent probes, the existing substituents on the core of coumarin compounds were modified. Based on the positions of the modified substituents, some of the fluorescent probes reported in the past ten years are listed. Most of the fluorescent probes are formed by modifying the 3 and 7 position substituents on the mother nucleus, and the 4 and 8 position substituents are relatively less modified. In terms of probe applications, the detection and application of coumarin fluorescent probes for Cu<sup>2+</sup>, Hg<sup>2+</sup>, Mg<sup>2+</sup>, Zn<sup>2+</sup>, pH, environmental polarity, and active oxygen and sulfide in the past ten years are mainly introduced.

Received 9th December 2019

Accepted 15th February 2020

DOI: 10.1039/c9ra10290f

rsc.li/rsc-advances

## 1. Introduction

In contrast to the general instrumental methods, fluorescence analyses have many outstanding features under physiological conditions, such as high sensitivity<sup>1,2</sup> or selectivity,<sup>2,3</sup> simple manipulations,<sup>4,5</sup> low cost,<sup>5</sup> rapid response rate,<sup>6</sup> real-time detection,<sup>7</sup> spatiotemporal resolution<sup>8</sup> and facile visualization.<sup>9,10</sup> In the past decade, a wide variety of fluorescent probes with different recognition moieties have been designed, which were based on the most versatile fluorophores, including fluorescein,<sup>11</sup> coumarin, cyanine,<sup>12</sup> boron-dipyrromethene (BODIPY),<sup>13</sup> rhodamine, and 1,8-naphthalimide.<sup>14–17</sup> They are usually used to detect various analytes. Therefore, the current study on fluorescence probes is a hot topic.

Coumarin, also known as benzopyran-2-one, is widely found in nature. It belongs to the flavonoid class of plant secondary metabolites and has a variety of biological activities, usually associated with low toxicity.<sup>18,19</sup> Coumarin is widely distributed in different parts of plants and has the highest concentration in fruits, seeds, roots and leaves.<sup>20–22</sup> It was first isolated from

Tonka beans in 1820 and the first synthesis was reported in 1882.<sup>23</sup> Various coumarin derivatives synthesized by modifying the structure of benzopyran ring show different pharmacological activities and they are widely used in medicine field. Coumarin derivatives can be used as fluorescent probes for metal ions due to their highly variable size, hydrophobicity, and chelation. The use of coumarin as a fluorescent probe began in the 19th century. Coumarin fluorescent probes have been widely used in many fields such as environmental protection and medicine. For example, Jun-Wu Chen *et al.* synthesized a fluorescent probe **1** (Fig. 1) composing coumarin as a fluorophore and a vinyl ether group as recognition unit to detect the concentration of Hg<sup>2+</sup> in water. This probe reacts with Hg<sup>2+</sup> to produce a strong fluorescence even the concentration of Hg<sup>2+</sup> is lower than 2 ppm (Hg<sup>2+</sup> concentration limits for drinking water set by the U.S. Environmental Protection Agency).<sup>24</sup> So that, it can be used to monitor water pollutions.<sup>25</sup> In medicine, coumarin fluorescent probes can be used for intracellular biological imaging, which can then be used to detect some cancers.

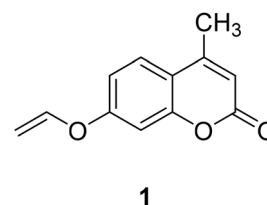


Fig. 1 The structure of compound 1.

<sup>a</sup>School of Medicine and Life Sciences, University of Jinan, Shandong Academy of Medical Sciences, Jinan 250200, Shandong, China. E-mail: 1226731832@qq.com; 871534141@qq.com; 1172493743@qq.com

<sup>b</sup>Institute of Materia Medical, Shandong First Medical University & Shandong Academy of Medical Sciences, Jinan 250062, Shandong, China. E-mail: liuteng823@163.com; Sunjie310@126.com; xiaojing6@gmail.com

<sup>c</sup>Key Laboratory for Biotech-Drugs Ministry of Health, Jinan 250062, Shandong, China

<sup>d</sup>Key Laboratory for Rare & Uncommon Diseases of Shandong Province, Jinan 250062, Shandong, China



To date, medical imaging has made great advances in locating and discriminating tumor lesions.<sup>26</sup> Hong Y. Song synthesized the coumarin fluorescent probe **2** (Fig. 2), to label a bioactive small peptide bearing a cysteine sulfhydryl group. The arginine–glycine–aspartic acid (Arg–Gly–Asp; RGD) ligand has a high affinity with the integrin  $\alpha v\beta 3$  receptor which is up-regulated on some tumor cell membranes and plays an important role in metastasis.<sup>27</sup> This peptide has also been radio-labelled for PET imaging of tumors.<sup>28</sup>

At present, the luminescence mechanism of most coumarin fluorescent probes can be divided into PET,<sup>29</sup> ICT,<sup>30,31</sup> FRET.<sup>32</sup>

## 2. Luminescence mechanism of coumarin fluorescent probes

### 2.1 PET mechanism (Fig. 7)

A typical PET system is constructed by attaching the recognition group R (receptor), which contains the electron donor, to a F (fluorophore) through S (spacer) (Fig. 3).<sup>33</sup>

Currently, most PET fluorescent probes have been reported to use fat amino or azacrown ether as the identification group, like structure **3**<sup>34</sup> (Fig. 4) and structure **4**<sup>35</sup> (Fig. 5).

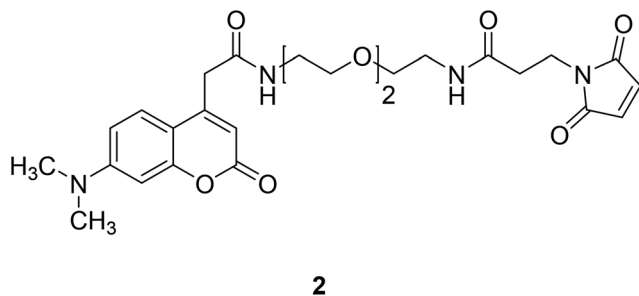


Fig. 2 The structure of compound **2**.

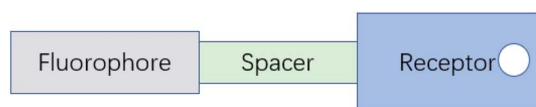


Fig. 3 The "fluorophore–spacer–receptor" format of fluorescent PET.<sup>33</sup> (Picture from ref. 33).

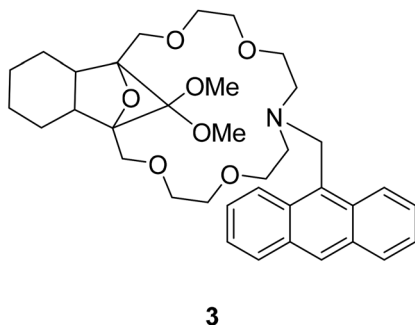


Fig. 4 The structure of compound **3**.

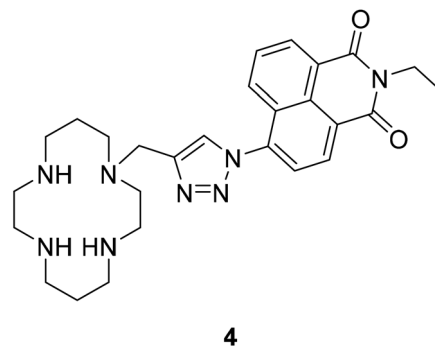


Fig. 5 The structure of compound **4**.

Most PET fluorescent probes are designed to bind the receptor to the object, inhibiting the light-induced electron transfer and causing the fluorophore to emit intense fluorescence (Fig. 6a). However, when interacting with the transition metal, the electrons can be transferred from the fluorophore to the transition metal or from the transition metal to the fluorophore due to the Redox behavior of the 3d electrons of the transition metal, resulting in fluorescence quenching by no radiation energy transfer (Fig. 6b).<sup>36</sup>

Styliani Voutsadaki *et al.* synthesized a turn on PET fluorescent sensor **5** (Fig. 8) selective for  $\text{Hg}^{2+}$  ions in aqueous in 2010.<sup>38</sup> Electrons of this probe are transferred from crown ether to the fluorophore and the fluorescence is attenuated.<sup>39</sup> This process is cancelled when it bonds with metal ion, and the fluorescence intensity increases with the increase of metal concentration. This probe is potential to detect and quantify mercury in environmental and biological samples.

Yu Xu *et al.* synthesized compound **6** (Fig. 9) which synthetic mechanism is PET in 2014.<sup>40</sup> This probe responds to pH by fluorescence quenching at 460 nm in the fluorescence spectrum, or by the ratio of maximum absorbance at 380 nm to 450 nm in the UV-visible spectrum, showing high sensitivity. In addition, probe **6** can monitor pH changes in real time because its fluorescence intensity is reversible between pH 1 and pH 7.

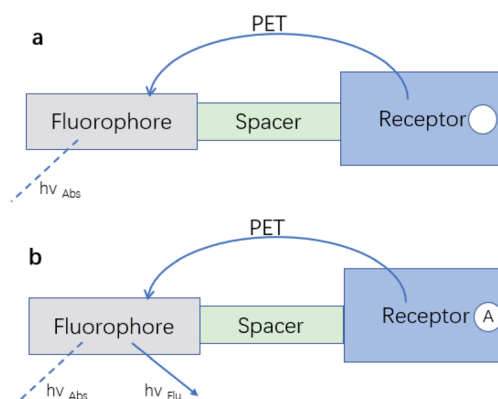


Fig. 6 (a) An electron transfer from the analyte-free receptor to the photo-excited fluorophore creates the "off" state of the sensor. (b) The electron transfer from the analyte-bound receptor is blocked resulting in the "on" state of the sensor.<sup>33</sup> (Picture from ref. 33).

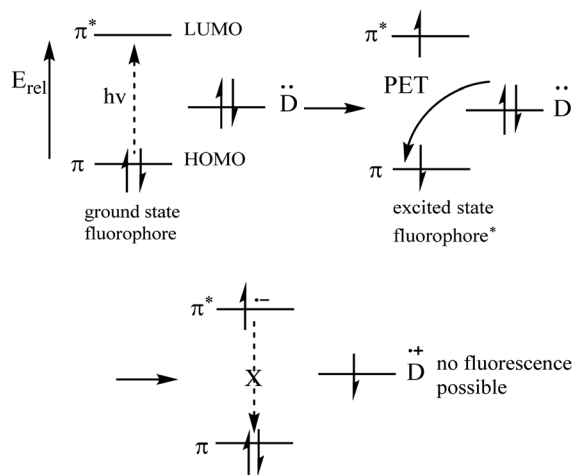


Fig. 7 Molecular orbital energy diagrams<sup>37</sup> (Picture from ref. 37).

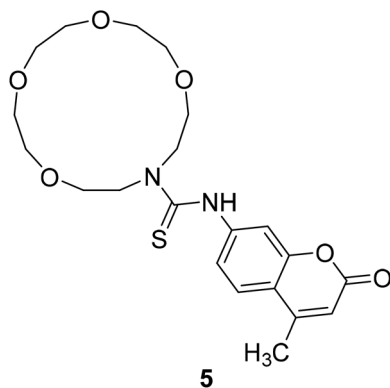


Fig. 8 The structure of compound 5.

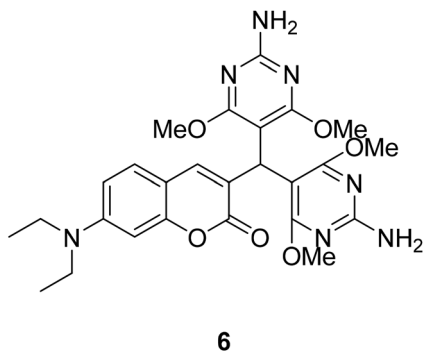


Fig. 9 The structure of compound 6.

Furthermore, this probe could be an ideal pH indicator for strongly acidic conditions with good biological significance.

Long Yi *et al.* reported a thiol probe 7 (Fig. 10) based on the photoinduced electron transfer (PET) effect in 2009.<sup>41</sup> The reaction of compound 7 with mercaptan produces blue-green emission visible to the naked eye. Thus, compound 7 can be used as a quantitative thiol probe for potential biological applications.

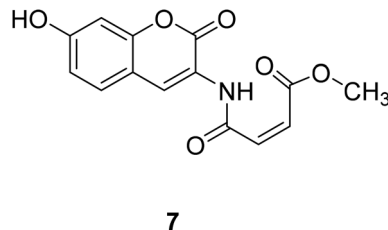


Fig. 10 The structure of compound 7.

Kyung-Sik Lee *et al.* reported a coumarin-based fluorescent probe 8 (Fig. 11) in which the nitrogen's lone pair of electrons of the ring thiazolidine and *ortho*-hydroxy group form a hydrogen bond, preventing the quenching of PET and showing high selectivity to Hcy and Cys.<sup>42</sup>

## 2.2 ICT mechanism (Fig. 12)

The ICT fluorescent molecular probe is composed of a fluorophore, a strongly attracted electron base and a strongly pushed electron base, conjugated to form a strong push-pull electron system. Under photoexcitation, it will be generated the charge transfer from the electron donor to the electron acceptor. The combination of the identification group of the ICT fluorescence probe with the object affects the push-pull electron effect of the fluorophore, weakens or strengthens the intramolecular charge transfer, and thus leads to changes of the fluorescence spectrum, such as blue shift or red shift.<sup>43</sup>

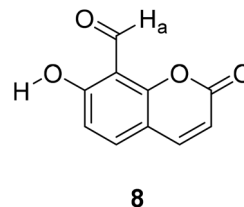


Fig. 11 The structure of compound 8.

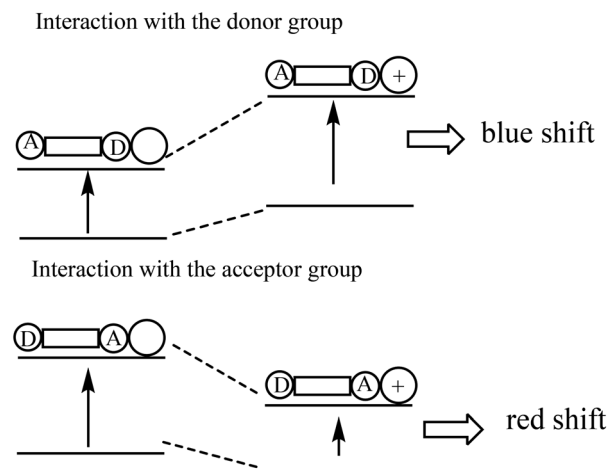


Fig. 12 Intramolecular conjugate charge transfer principle<sup>43</sup> (Picture from ref. 43).



Compound **9** (Fig. 13) reacts with  $\text{H}_2\text{S}$ , exhibits an increase absorbance at 405 nm. The interaction increased the push–pull character and resulted the large bathochromic shifts in the absorption and the ICT effect.<sup>44</sup>

Jun Li *et al.* designed and synthesized the plasma probe **10** (Fig. 14) based on the intramolecular charge transfer (ICT) mechanism for the detection of bio thiols in aqueous solution in 2013.<sup>45</sup> The probe **10** itself has weak fluorescence, but shows strong fluorescence when combined with  $\text{R}_2\text{SH}$ .

### 2.3 FRET mechanism

The fluorescent probe which based on FRET mechanism can join two fluorophores (donor and acceptor) in one molecule.<sup>36</sup> Donor (D) collect radiation at the excitation wavelength and transfer this energy to the acceptor (A), which emits it at a longer wavelength. When the emission spectrum of the donor overlaps the absorption spectrum of the acceptor, it may occur non-radiative energy transfer from D to A. When D is excited, we

can observe the fluorescence emission of A owing to energy transfer.

A. E. Albers *et al.* synthesized a fluorescent probe **11** (Fig. 15) for quantitative detection of endogenous  $\text{H}_2\text{O}_2$  in 2006.<sup>46</sup> The spectral overlap between luciferin absorption and coumarin release of **11** was very small, and the fluorescence energy transfer (FRET) was inhibited, so only blue donor emission was observed. When **11** interacts with  $\text{H}_2\text{O}_2$ , the spectral overlap increases, and the green fluorescein receptor is increased by FRET emission, excitation at 420 nm produces a bright green-colored fluorescence, so changes in  $[\text{H}_2\text{O}_2]$  can be detected by measuring the ratio of blue to green fluorescence intensity.

Changyu Zhang synthesized a coumarin fluorescent probe **12** (Fig. 16) based on the FRET mechanism in 2015 for the detection of  $\text{H}_2\text{S}$  with high sensitivity.<sup>47</sup>

Fluorescence analysis has many outstanding characteristics under physiological conditions, such as high sensitivity, strong selectivity, simple operation, low cost, fast response speed, real-time detection, high spatiotemporal resolution, and convenient visualization. Currently, more fluorescent probes are reported. The light-emitting mechanism is based on PET, ICT, and FRET mechanisms. These three mechanisms all have certain disadvantages, such as low sensitivity, poor selectivity, and high environmental requirements required for the probe to function. Compared with the other two, the design of the ratio probe using the fluorescence resonance energy transfer (FRET) mechanism has many advantages, which can reduce the fluorescence detection error and self-quenching.

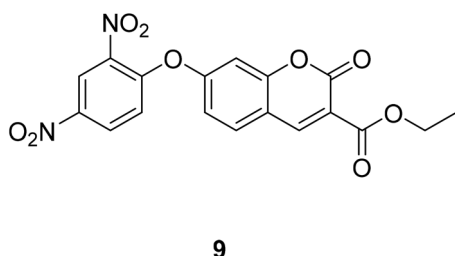


Fig. 13 The structure of compound **9**.

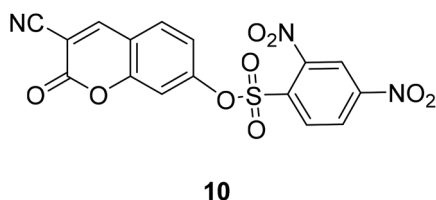


Fig. 14 The structure of compound **10**.

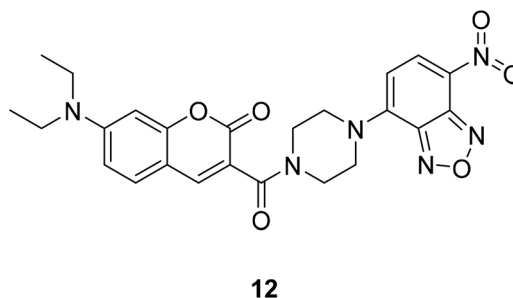
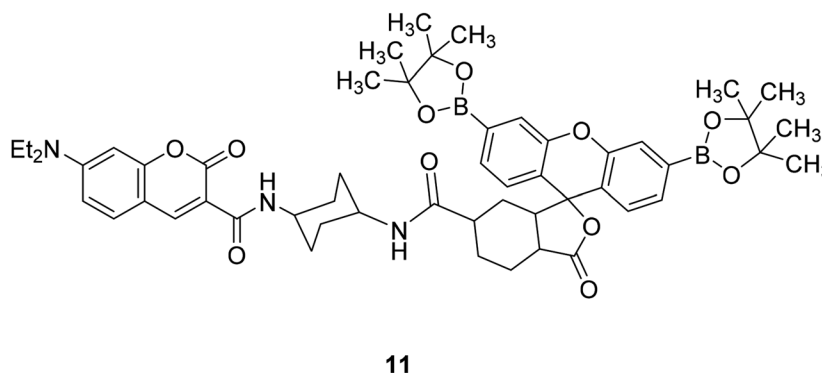
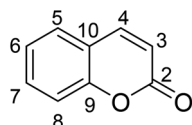


Fig. 16 The structure of compound **12**.



### 3. Synthesis of coumarin fluorescent probes

The synthesis of coumarin fluorescent probes is a popular topic in recent years. Their synthesis is partly based on classical methodologies such as Pechmann reaction or Knoevenagel condensation, but it also sparked the discovery of completely new pathways.<sup>48</sup> The synthesis of coumarin fluorescent probe is



13

Fig. 17 The chemical structure and numbering scheme of coumarin.

based on the existing coumarin for the derivation, by changing the substituents to make the derivative have fluorescence characteristics, thus become a fluorescent probe in some aspects. Based on the classification of substituent position on the parent nucleus of coumarin, this paper introduced the synthesis methods of some fluorescent probes reported in this decade. Of course, it mainly introduced the synthesis of coumarin fluorescent probes mainly based on the three most common fluorescent luminescence mechanisms (PET, ICT and FRET) (Fig. 17).

#### 3.1 Classification by substituent position

**3.1.1 Modification of the 3-position substituent of coumarin.** Yu Xu *et al.* modified the 7-substituent of compound 14 to synthesize compound 6 which can be used to detect ambient pH in 2014 (Fig. 18).<sup>40</sup>

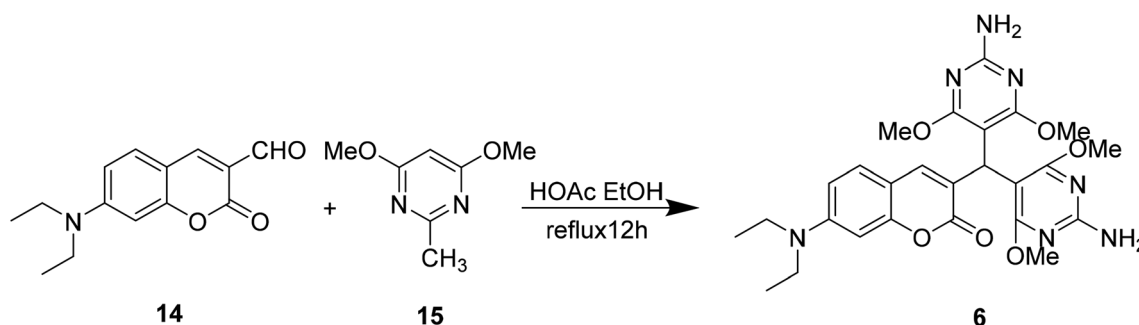


Fig. 18 The synthetic route of compound 6.

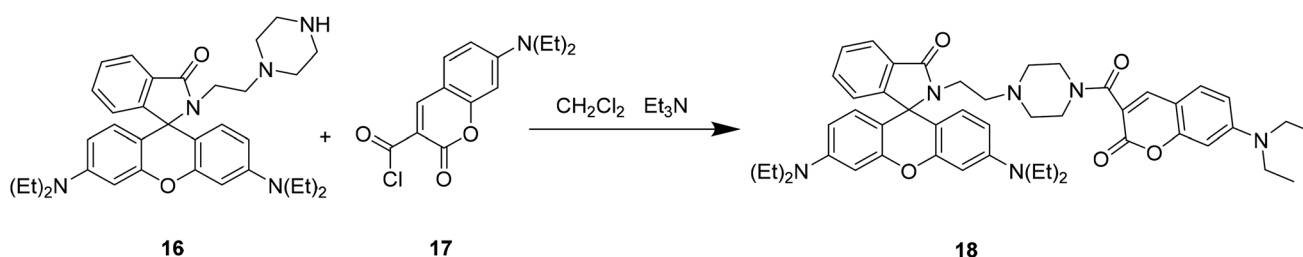


Fig. 19 The synthetic route of compound 18.

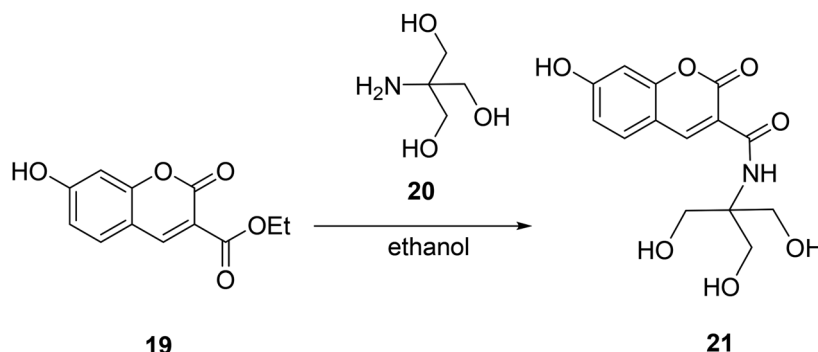


Fig. 20 The synthetic route of compound 21.



Xiao-Fan Zhang *et al.* modified the substituent at the 3-position of compound **16** to develop a coumarin-rhodamine fluorescent probe **18** as a pH probe in 2013 (Fig. 19).<sup>49</sup>

Da En modified the 3-position substituent of compound **19** and designed a fluorescent probe **21** with high sensitivity and selectivity for Fe<sup>3+</sup> ions in cells in 2014 (Fig. 20).<sup>50</sup>

Ying-Che Chen modified the substituent at position 3 of compound **22** to form a fluorescent probe **24**. The fluorescent probe **24** binds to a target protein labeled with a short peptide sequence containing two Cys residues, which causes fluorescence quenching (Fig. 21).<sup>51</sup>

Qi-Hua You modified the 3-position substituent of the compound **25** and designed a fluorescent probe **27** for detecting copper ions with good selectivity and sensitivity in 2014 (Fig. 22).<sup>52</sup>

**3.1.2 Modification of the 4-position substituent of coumarin.** Kai-Bo Zheng *et al.* developed a fluorescent probe **29**

in 2014 which contains heavy atomic palladium, and should not display fluorescence, but interacts with CO to induce the release of palladium and restore fluorescence, showing a new emission band at 477 nm. Compound **29** has a higher sensitivity and an 11-fold increase in signal strength compared to current CO probes. The detection limit is  $6.53 \times 10^{-7}$  M (Fig. 23).<sup>53</sup>

**3.1.3 Modification of the 7-position substituent of coumarin.** Styliani Voutsadaki *et al.* modified the 3-position substituent of compound **31** to synthesized a “turn on” fluorescent sensor **5** selective for Hg<sup>2+</sup> ions in aqueous in 2010 (Fig. 24).<sup>54</sup>

Xiao-Wei Cao *et al.* designed compound **35** to detect F<sup>−</sup> by modifying the 7-position substituent of compound **34** in 2011 (Fig. 25).<sup>54</sup>

Danbi Jung, in 2014, modified a 7-position substituent on compound **36** to synthesize a fluorescent probe **38**, which can be

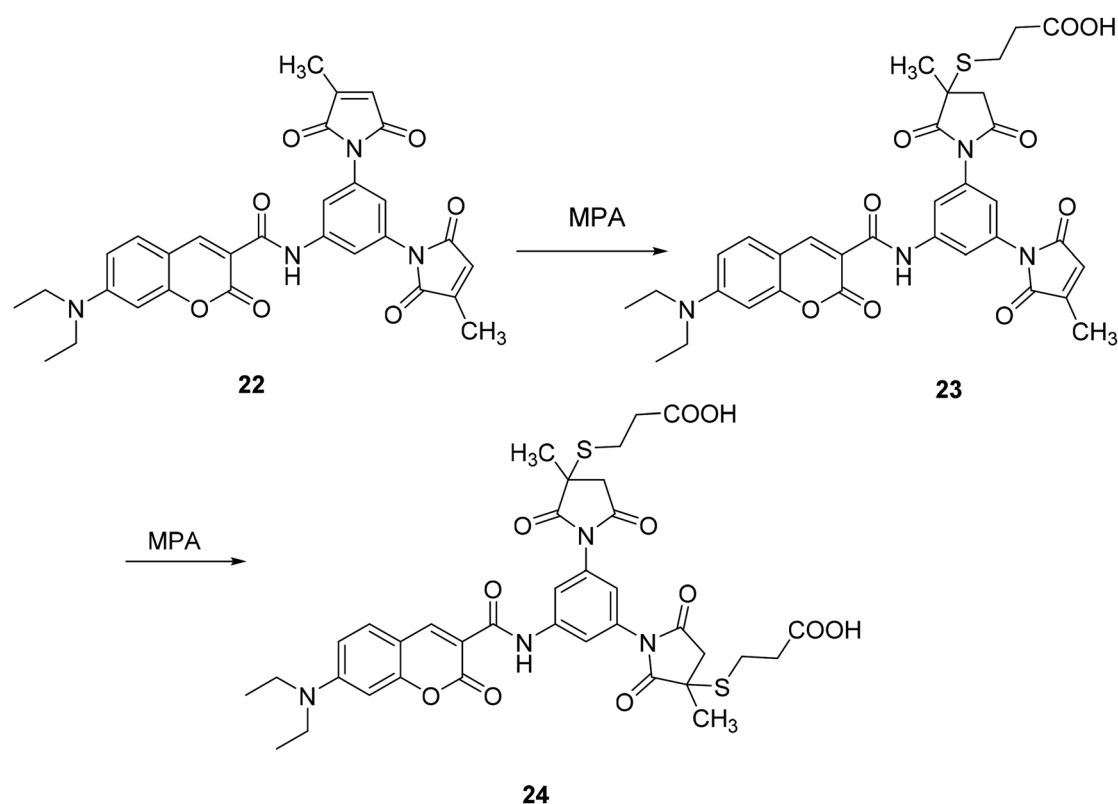


Fig. 21 The synthetic route of compound **24**.

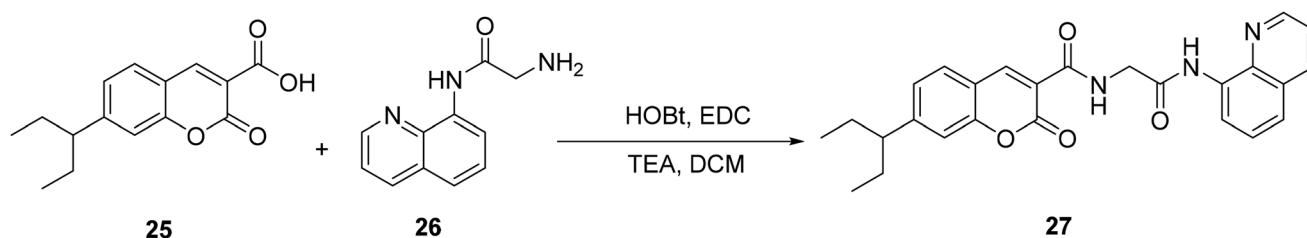


Fig. 22 The synthetic route of compound **27**.

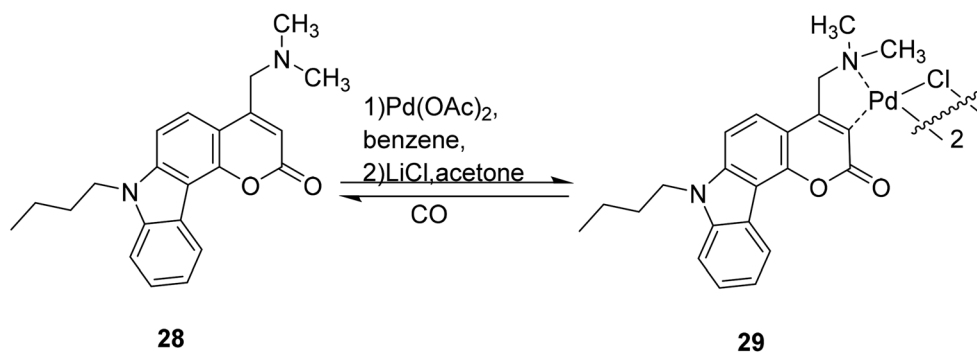


Fig. 23 The synthetic route of compound 29.

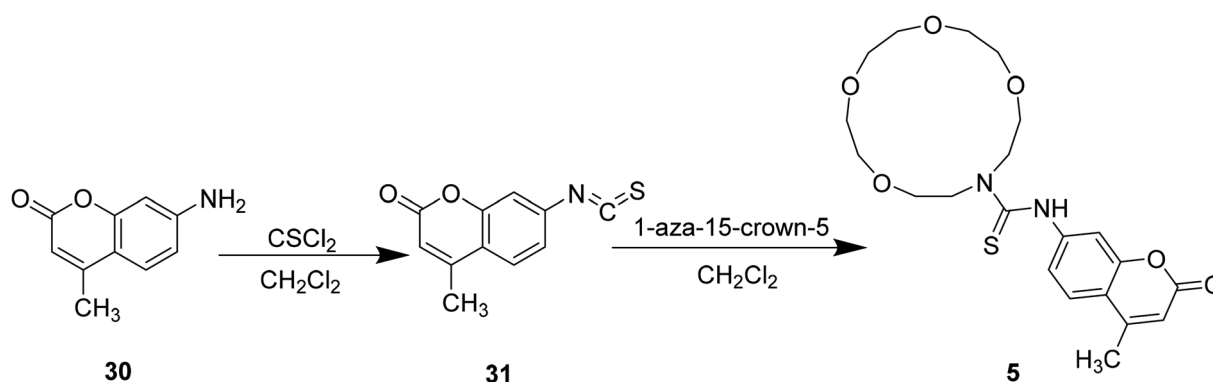


Fig. 24 Synthesis of compound 5.

used to monitor thiol levels in cancer cells by fluorescence imaging, which is practical (Fig. 26).<sup>55</sup>

**3.1.4 Modification of the 8-position substituent of coumarin.** Mi-hui Yan synthesized probe **40** in 2011 by modifying the 8-position substituent of compound **39**. Probe **40** is fluorescently turned on for zinc ions and has good selectivity (Fig. 27).<sup>56</sup>

In the study of the modification of the coumarin core structure to prepare fluorescent probes, we can find that most of the fluorescent probes are modified by the 3 and 7 substituents on the coumarin core structure. There were relatively few probes obtained by modifying the 4- and 8-position substituents (Table 1).

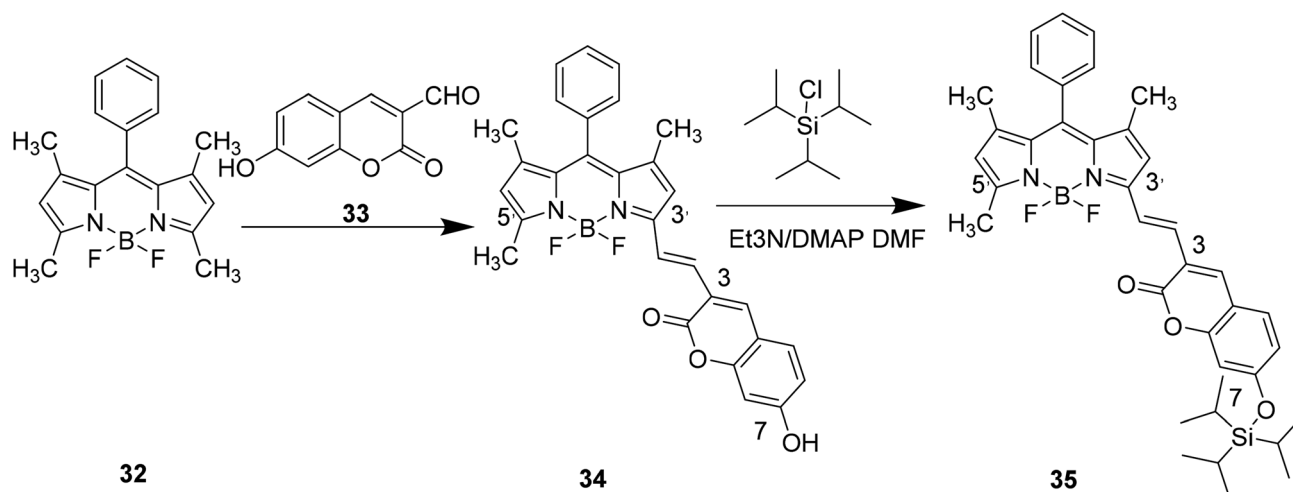
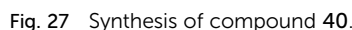
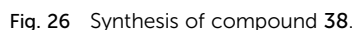


Fig. 25 Synthesis of compound 35.







Metal ion fluorescent probes have important applications in many fields such as environmental protection, biomedicine, chemistry, *etc.* In terms of environmental protection, heavy metal ion pollution has become increasingly serious in recent years, so it is particularly important to detect the concentration and content of heavy metal ions in the environment effectively, simply and quickly. Therefore, the development of a heavy metal ion fluorescence probe for indicating environmental pollution has great research value. In biomedical, since many metal ions take part in some important biochemical reactions in the body, or participate in the formation of coenzymes,<sup>58</sup> as signal molecules to affect normal physiological functions, the form of some metal ions concentration in the body can reflect some chemical reaction process, and as a basis for the disease diagnosis, and indicated the development process of the



**Table 1** The coumarin fluorescent probe structure and fluorescent indicator of "application" part

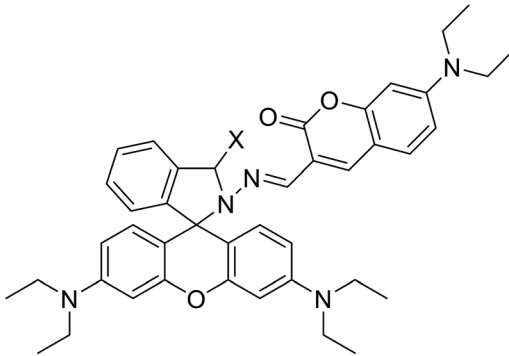
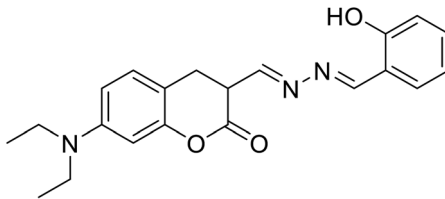
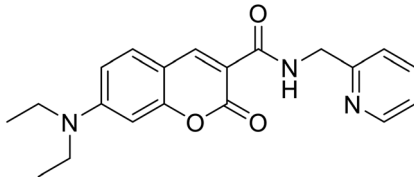
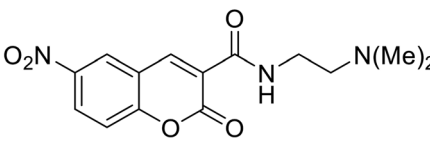
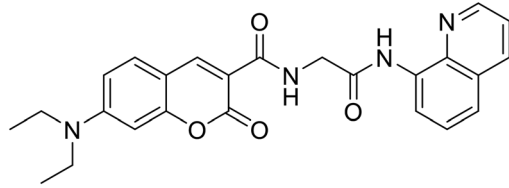
Fluorescent probe type		Probe structure	Change in fluorescence	Location of coumarin functionalization
Metal ion fluorescent probe	Reacts with $\text{Cu}^{2+}$	 <p><b>41: X=O</b> <b>42: X=S</b></p>	<p><b>41:</b> Fluorescence changed from yellow to bright red</p> <p><b>42:</b> Show strong orange fluorescence at 590 nm</p>	3-Position
		 <p><b>43</b></p>	Fluorescence quenching	3-Position
		 <p><b>44</b></p>	Show fluorescence enhancement	3-Position
		 <p><b>45</b></p>	Show fluorescence enhancement	3-Position
		 <p><b>46</b></p>	"Turn-on" probe; from no fluorescent to fluorescent	3-Position



Table 1 (Contd.)

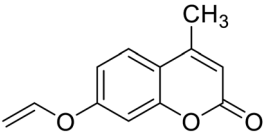
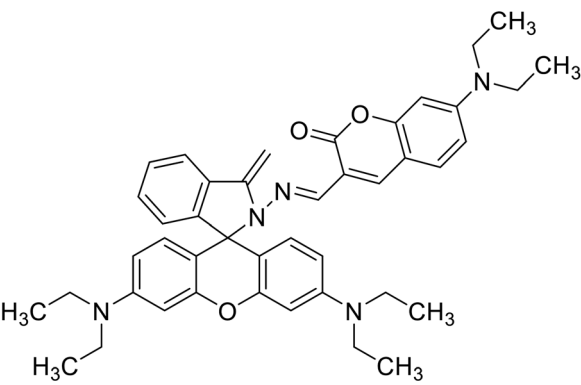
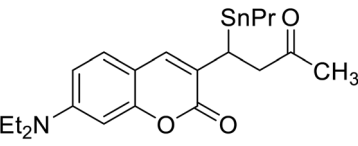
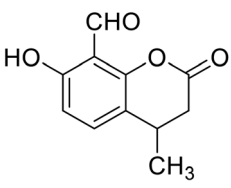
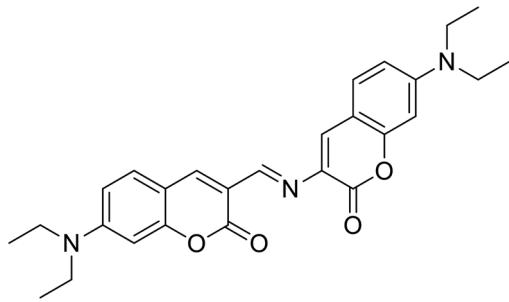
Fluorescent probe type	Probe structure	Change in fluorescence	Location of coumarin functionalization
Reacts with $\text{Hg}^{2+}$	 <b>1</b>	Show strong blue fluorescence	7-Position
	 <b>47</b>	Show a reversible dual chromo- and fluorogenic response	3-Position
	 <b>48</b>	Show fluorescence enhancement	3-Position
Reacts with $\text{Mg}^{2+}$	 <b>49</b>	Fluorescence changed from weak blue to bright blue	7-Position and 8-position
	 <b>50</b>	Fluorescence changed from non to strong red	3-Position



Table 1 (Contd.)

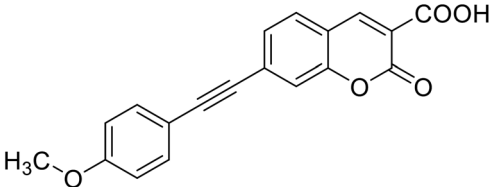
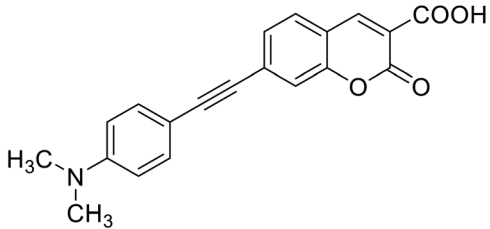
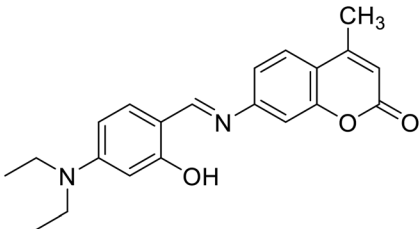
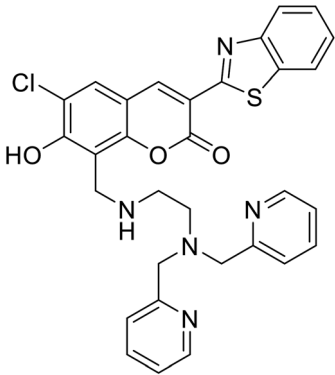
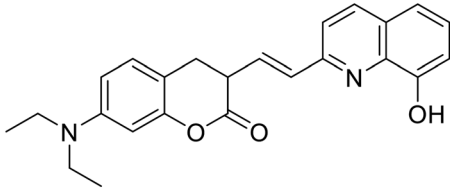
Fluorescent probe type	Probe structure	Change in fluorescence	Location of coumarin functionalization
Reacts with $Zn^{2+}$	 <p>51</p>	Show fluorescence enhancement	3-Position
	 <p>52</p>	Show fluorescence enhancement	3-Position
	 <p>53</p>	Show significant increase in fluorescence at 500 nm	7-Position
pH fluorescent probe	 <p>54</p>	Absorption spectrum shifted toward longer wavelengths, and the fluorescence is enhanced	7-Position and 8-position
	 <p>55</p>	As the pH decreased, the absorption spectrum gradually red-shifted	3-Position



Table 1 (Contd.)

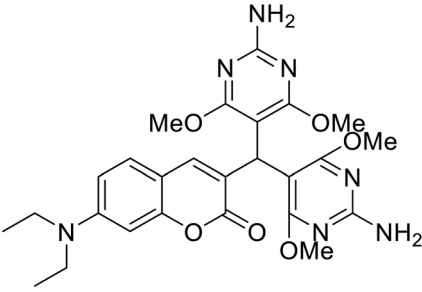
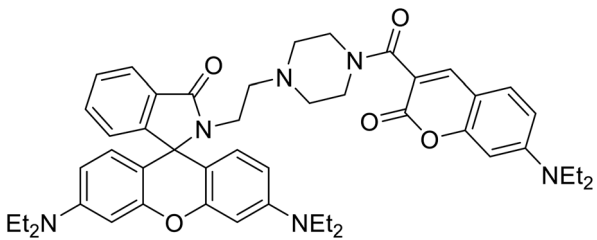
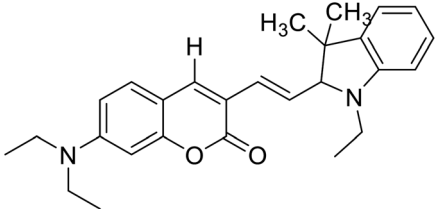
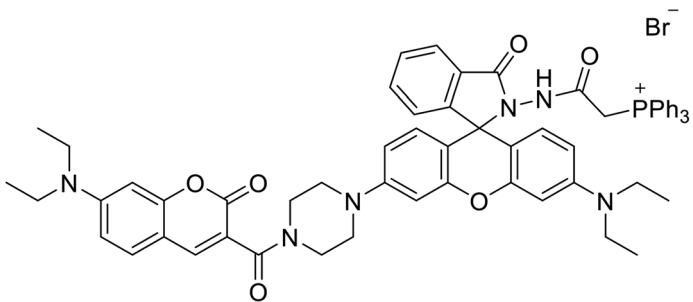
Fluorescent probe type	Probe structure	Change in fluorescence	Location of coumarin functionalization
	 <b>6</b>	When the pH is low (below 3.5), the fluorescence at 460 nm is quenched	3-Position
	 <b>18</b>	When the probe interacted with H <sup>+</sup> , the coumarin release decreased at 477 nm and the rhodamine release increased at 582 nm	3-Position
Oxygen and sulfide fluorescent probes	Reacts with oxygen		
	 <b>56</b>	$I_{651}/I_{495}$ increased significantly	3-Position
	 <b>57</b>	New emission appeared at 580 nm. The emission intensity increased with the increase of hypochlorite dose, and the fluorescence intensity decreased at 470 nm	3-Position



Table 1 (Contd.)

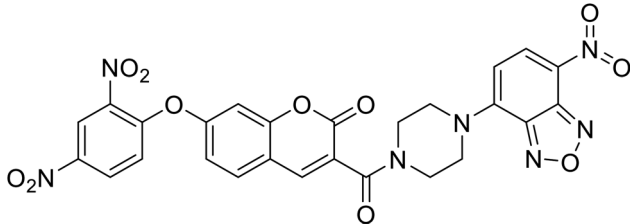
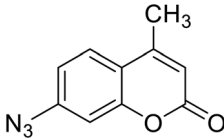
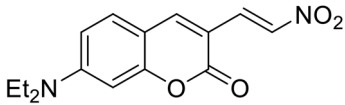
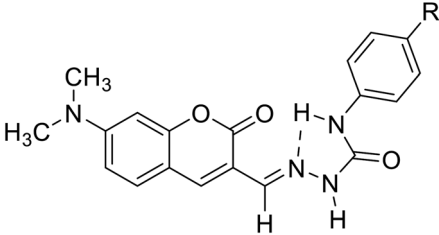
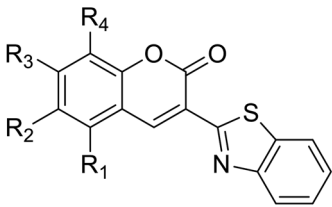
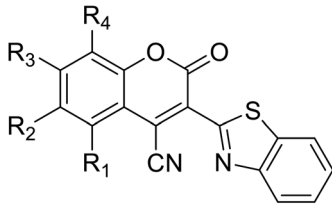
Fluorescent probe type	Probe structure	Change in fluorescence	Location of coumarin functionalization
Reacts with $H_2S$	 <p style="text-align: center;"><b>58</b></p>	Fluorescence quenching	Functionalized position of fluorescent probe based on FRET mechanism: 3-position Functionalized position of fluorescent probe based on ICT mechanism: 7-position
	 <p style="text-align: center;"><b>59</b></p>	Show fluorescence enhancement	7-Position
	 <p style="text-align: center;"><b>60</b></p>	Generates a large emission displacement	3-Position
Environmental polarity probes	 <p style="text-align: center;"> <b>61</b>  <b>62</b>  <b>63</b>  <b>64</b> </p> <p style="text-align: center;"> R=-CN  =-CF<sub>3</sub>  =-F  =-OCH<sub>3</sub> </p>	Show orange-yellow colour change and simultaneous fluorescence increase	3-Position



Table 1 (Contd.)

Fluorescent probe type	Probe structure	Change in fluorescence	Location of coumarin functionalization
	 <p><b>65a-d</b></p> <p>a: R<sub>1</sub>=R<sub>4</sub>=H, R<sub>2</sub>=R<sub>3</sub>=OMe  b: R<sub>1</sub>=R<sub>2</sub>=H, R<sub>3</sub>=R<sub>4</sub>=OMe  c: R<sub>1</sub>=R<sub>2</sub>=H, R<sub>3</sub>=R<sub>4</sub>=-OCH<sub>2</sub>CH(COOEt)-O-  d: R<sub>1</sub>, R<sub>2</sub>=fused phenyl ring, R<sub>3</sub>=R<sub>4</sub>=H</p>	When the polarity of environment decreases, it shows strong fluorescence	<b>66e-g:</b> 4-position
	 <p><b>66e-g</b></p> <p>e: R<sub>1</sub>=R<sub>4</sub>=H, R<sub>2</sub>=R<sub>3</sub>=OMe  f: R<sub>1</sub>=R<sub>2</sub>=H, R<sub>3</sub>=R<sub>4</sub>=OMe  g: R<sub>1</sub>=R<sub>2</sub>=H, R<sub>3</sub>=R<sub>4</sub>=-OCH<sub>2</sub>CH(COOEt)-O-</p>		

disease. Based on these important functions, the study of metal ion fluorescence probe is of great value. Coumarin derivatives can be used as fluorescent probes for metal ions because of their highly variable size, hydrophobicity, and chelation.<sup>59</sup>

**4.1.1 Cu<sup>2+</sup> fluorescence detection.** Copper are trace elements needed in the body, which assist many kinds of metalloenzymes to play a role. In humans, copper is essential to the proper functioning of organs and metabolic processes. It is a constituent of many enzyme systems like oxidases and hydroxylases.<sup>58</sup>

Maity and his group synthesized two fluorescence probes (**41** and **42**) (Fig. 28) to detect selectively Cu<sup>2+</sup> ions in aqueous buffer medium in 2013.<sup>59</sup> Selected 480 nm as the excitation

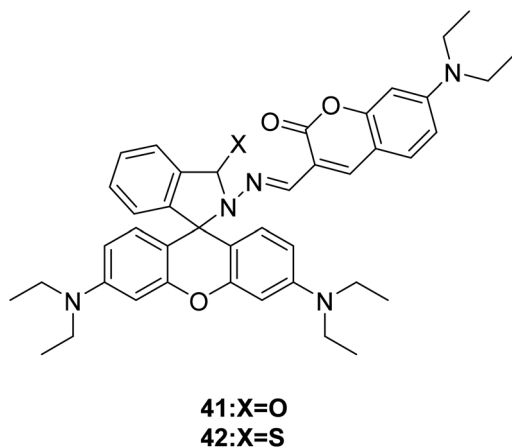


Fig. 28 The structure of compound 41 and 42.

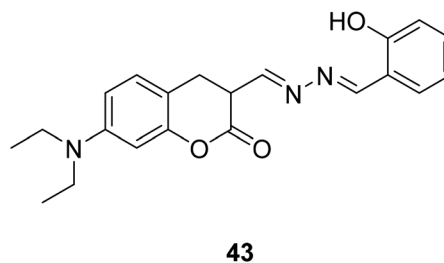


Fig. 29 The structure of compound 43.



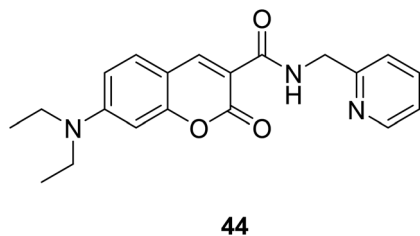


Fig. 30 The structure of compound 44.

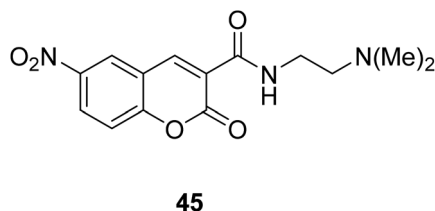


Fig. 31 The structure of compound 45.

wavelength, the ring of rhodamine–thiolactam was partially opened with the addition of  $\text{Cu}^{2+}$ , the yellow colored probe **41** changed to bright red upon  $\text{Cu}^{2+}$ , probe **42** showed strong orange fluorescence at 590 nm.

Jiun-Ting Yeh *et al.* synthesized a new coumarin-derived fluorescent probe **43** (Fig. 29) exhibited significant fluorescence quenching in the presence of  $\text{Cu}^{2+}$  ions in 2014.<sup>60</sup> The maximum fluorescence quenching occurred over a pH range of 5–9. This coumarin-based  $\text{Cu}^{2+}$  chemosensor serves as an effective and non-destructive probe for  $\text{Cu}^{2+}$  detection in living cells. And it also can be used in the area of environmental protection and food safety.

Hyo Sung Jung *et al.* developed a novel fluorogenic probe **44** (Fig. 30) bearing the 2-picolyl unit with high selectivity and suitable affinity toward  $\text{Cu}^{2+}$  in biological systems in 2009.<sup>64</sup> The receptor can monitor  $\text{Cu}^{2+}$  ion in aqueous solution with a pH span 4–10. The compound **44** can be used for the fluorescence microscopic imaging and the study on the biological functions of  $\text{Cu}^{2+}$ . Ahmadreza Bekhradnia *et al.* synthesized a novel fluorescent chemo sensor: coumarin carboxamide **45** (Fig. 31), through microwave irradiation in 2016.<sup>62</sup> The compound can be used as fluorescent probe for  $\text{Cu}^{2+}$  with selectivity over other metal ions in aqueous solution and exhibit enhanced fluorescence. Rapid detection of  $\text{Cu}^{2+}$  ions in water plays an important role in improving environmental pollution.<sup>63</sup>

Qi-Hua You *et al.* synthesised a coumarin-based fluorescent chemo sensor **46** (Fig. 32) in 2014.<sup>52</sup> It can recognize  $\text{Cu}^{2+}$  in aqueous acetonitrile solutions with high selectivity and sensitivity. Using the Cu-containing complex **46**– $\text{Cu}^{2+}$  as a sensing ensemble, highly selective recognize His/bio thiols. It also can be applied in fluorescence imaging of histidine in hard-to-transfect living cells. Due to its intrinsic paramagnetic properties,  $\text{Cu}^{2+}$  can quench the fluorescence of fluorescent metal chelators to make ensemble devices in nonfluorescence off state.<sup>64</sup> Then, effectively snatch  $\text{Cu}^{2+}$  ions through  $\text{Cu}^{2+}$ -binding

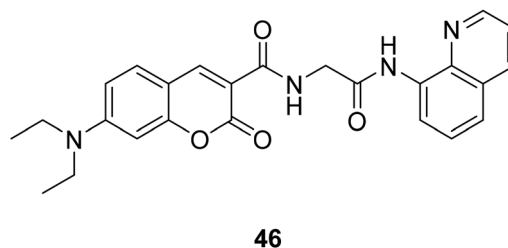


Fig. 32 The structure of compound 46.

analyte from the ensemble in aqueous solution can switch on the “turn-on” fluorescence of the sensing ensemble.<sup>65,66</sup>

**4.1.2  $\text{Hg}^{2+}$  fluorescence detection.**  $\text{Hg}^{2+}$  is a kind of heavy metal ion, can cause serious pollutions to the global environment.  $\text{Hg}^{2+}$  is a caustic and carcinogenic material with high cellular toxicity.<sup>67</sup> It easily change to the highly toxic methyl mercury, passes through biological membranes resulting in the human's neurological system damage, DNA damage, various cognitive and motion disorders,<sup>68</sup> and it can cause brain damage and other chronic diseases.<sup>69</sup> Therefore, research a method to monitor  $\text{Hg}^{2+}$  in many scientific fields, including medicine, environmental and the like, has significant meaning.<sup>70</sup> At present, there have been a lot of researches on mercury sensors. It is undeniable that the construction of mercury sensors can contribute to the preparation of other metal sensor. However, it must be admitted that its current application is very limited. Therefore, the breakthrough in the application of mercury sensor in the future is still the direction of efforts.

Chen-Jun Wu *et al.* synthesized a novel probe **1** in 2017 (ref. 25) which treated with  $\text{Hg}^{2+}$  in HEPES buffer solution shows remarkable fluorescence enhancement,<sup>71–73</sup> we can easily observe strong blue fluorescence by naked eyes. This method is sensitive and selective, so that it reveals the probe **1** could be used as a convenient tool to monitor  $\text{Hg}^{2+}$  in neat aqueous solution by fluorescence turn-on response. On the basis of the signal-to-noise ratio of three, the detection limit of this  $\text{Hg}^{2+}$  probe is determined as 0.12  $\mu\text{M}$  (24 ppb). It is lower than the majority of reported probes.<sup>73–77</sup> (According to the US EPA requirement, the limit of  $\text{Hg}^{2+}$  concentration for sake drinking water was set as 2 ppm). That means the probe **1** is sensitive enough to distinguish the  $\text{Hg}^{2+}$  for water quality detection.<sup>25</sup>

Qiu-juan Ma *et al.* synthesized a rhodamine–coumarin conjugate fluorescent probe **47** (Fig. 33) which with a sulfur-based functional group to detect  $\text{Hg}^{2+}$  in 2010.<sup>78</sup> In 50% water/ethanol buffered at pH 7.24, the probe **47** binds excess  $\text{Hg}^{2+}$  and sensing  $\text{Hg}^{2+}$  sensitively and selectively. Furthermore, because of the chelation-induced ring opening of rhodamine spiro lactam, probe **47** also showed a reversible dual chromo- and fluorogenic response toward  $\text{Hg}^{2+}$ . The development of  $\text{Hg}^{2+}$  ion fluorescence probes can be used to detect heavy metal pollution in the environment. It can be used to test the concentration of  $\text{Hg}^{2+}$  in both tap and river water samples.

Wei-Min Xuan and his groups reported a ratio-metric fluorescent probe **48** (Fig. 34) in 2012.<sup>79</sup> This probe can be used for





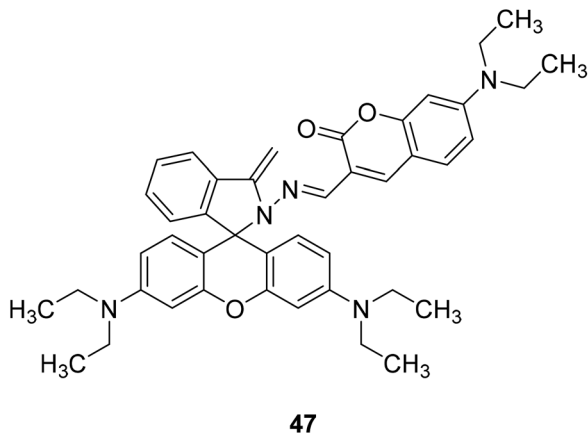


Fig. 33 The structure of compound 47.

living cell imaging and cell permeable. Even the concentration of  $\text{Hg}^{2+}$  was low as  $2 \times 10^{-8}$  M (close to the maximum contamination level set by the EPA), we can also observed pronounced fluorescent change.<sup>80</sup>

**4.1.3  $\text{Mg}^{2+}$  fluorescence detection.**  $\text{Mg}^{2+}$  is the most abundant divalent cation within cells and it plays an important physiological role in bone remodelling and skeletal development.<sup>81</sup> Magnesium deficiency may be related to the occurrence of many diseases, such as diabetes, osteoporosis, hypertension and coronary heart disease.<sup>82,83</sup>

Vinod Kumar Gupta *et al.* designed compound 49 (Fig. 35) in 2017 to detect  $\text{Mg}^{2+}$  in the presence of alkali and alkaline earth metal ions. It showed a significant fluorescence enhancement towards  $\text{Mg}^{2+}$ .<sup>84</sup> This probe has a low detection limit for  $\text{Mg}^{2+}$ . This probe is most widely used in Serum magnesium and the magnesium tolerance test. The fluorescence changes from weak blue to bright blue, which can be easily detected by the naked eye.<sup>82,84</sup>

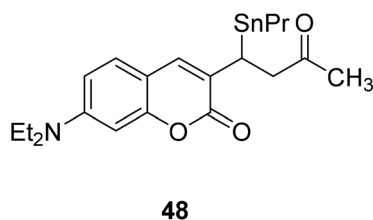


Fig. 34 The structure of compound 48.

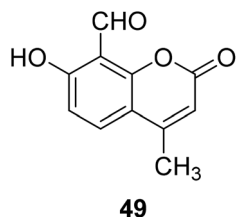


Fig. 35 The structure of compound 49.

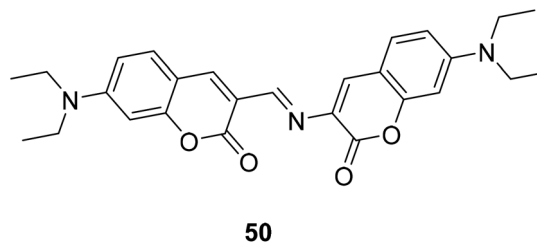


Fig. 36 The structure of compound 50.

Debdas Ray *et al.* designed a coumarin fluorescence sensors 50 (Fig. 36).<sup>85</sup> Which was designed to show a significant red fluorescence enhancement response to  $\text{Mg}^{2+}$ .

Hai-Jing Yin and his groups reported two novel 7-substituted coumarin-based two-photon fluorescent probes (51, 52) (Fig. 37) for biological  $\text{Mg}^{2+}$  detection in 2015. The probe has higher sensitivity, lower detection limit, and interacts with lower concentration of magnesium ions, showing enhanced fluorescence. The experiment found that these probes are not sensitive in the biologically relevant pH range and have low cytotoxicity, so we can apply them to physiological studies.<sup>86,87</sup>

**4.1.4  $\text{Zn}^{2+}$  fluorescence detection.**  $\text{Zn}^{2+}$  ions are involved in building enzymes and proteins and involved in a variety of biochemical reactions like gene transcription, regulation of metalloenzymes, neural signal transmission, superoxide dismutase, cytochrome oxidase.<sup>88–90</sup> Minute amounts of zinc help keep the body healthy, but too much can lead to bad results and disease. So as to keep health, it is really important to design several convenient tools to inspect the concentration of  $\text{Zn}^{2+}$ .

Jing-can Qin *et al.* synthesized a simple two-photon excitation (TPE) probe 53 (Fig. 38) for  $\text{Zn}^{2+}$  in 2016.<sup>91</sup> Two-photon excitation (TPE) has the advantages of reducing background fluorescence, increasing tissue penetration, and reducing light damage to biological samples, *etc.*<sup>92–94</sup> The probe selectively binds to zinc

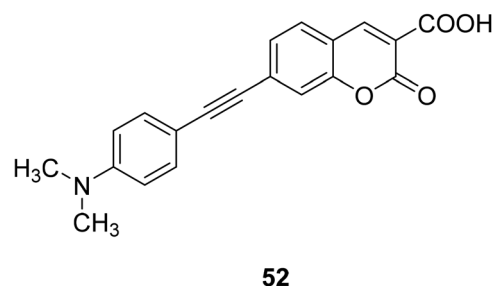
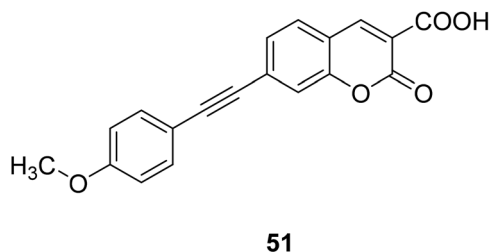
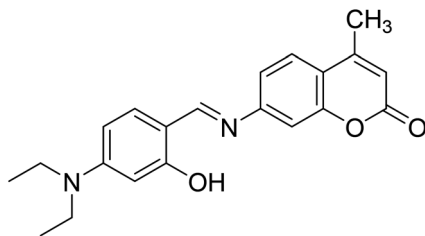


Fig. 37 The structure of compound 51, 52.



53

Fig. 38 The structure of compound 53.

ions, showing a significant increase in fluorescence at 500 nm. In addition, due to its low detection limit, the sensor should be able to find potential applications in detecting trace  $\text{Zn}^{2+}$  concentrations in biological systems and environments.<sup>91</sup>

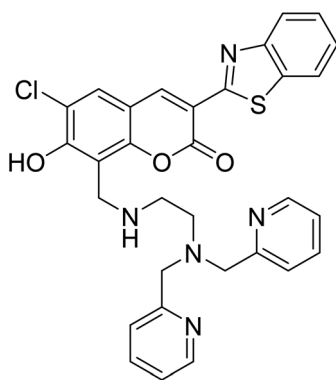
Shin Mizukami *et al.* designed a ratio-metric  $\text{Zn}^{2+}$  probe (54) (Fig. 39) in 2009.<sup>95</sup> The probe 54 could permeate living cell membranes, we introduced it to living RAW264 cells to observe the intracellular  $\text{Zn}^{2+}$  concentration *via* ratio metric fluorescence microscopy. When the probe is bound to zinc ions, the absorption spectrum shifted toward longer wavelengths, and the fluorescence is enhanced.

#### 4.2 Application in pH detection

Intracellular pH plays an important role in drug resistance, cell proliferation, invasion and metastasis, apoptosis, disease and other processes.<sup>96</sup> In addition, changes in intracellular pH have been linked to diseases such as some cancer and Alzheimer's disease.

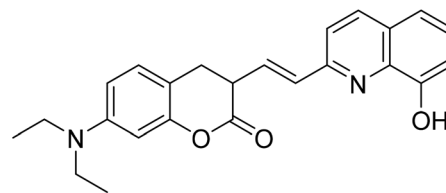
The fluctuation of pH has obvious effect on numerous cellular events, such as cellular metabolism,<sup>97</sup> cellular growth,<sup>98</sup> signal transduction,<sup>99</sup> chemotaxis, apoptosis,<sup>100</sup> and autophagy.<sup>101</sup> Therefore, monitoring pH changes inside living cells is crucial for exploring cellular functions and understanding physiological and pathological processes in organisms.

Sa-Sa Zhu *et al.* designed a new linked coumarin-quinoline ratio metric pH probe 55 (Fig. 40) which can be used in cellular



54

Fig. 39 The structure of compound 54.



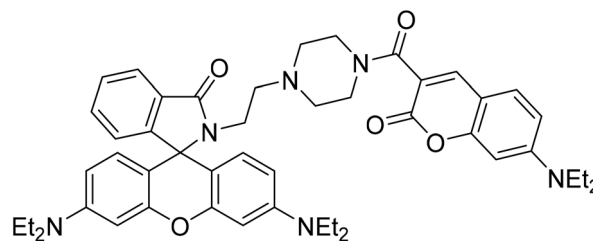
55

Fig. 40 The structure of compound 55.

imaging studies in 2013.<sup>102</sup> When the pH is from 7.4–2.9, the absorption peak of the probe near 425 nm is significantly reduced. At the same time, a new red-shifted absorption band was formed near 516 nm. As the pH decreased, the absorption spectrum gradually red-shifted. The characters of the novel probe include strong fluorescence under acidic conditions, low cytotoxicity and good cell membrane permeability; these features make the probe useful for monitoring pH variations from neutral to acidic conditions in living cells.

Yu Xu *et al.* synthesised a new turn-off fluorescent probe 6 (Fig. 9) with coumarin and imidazole moiety in 2014.<sup>40</sup> This probe could be a practical and ideal pH indicator and play a role in extremely acidic environments. When the pH is low (below 3.5), the fluorescence at 460 nm is quenched. A considerable number of microorganisms like *Helicobacter pylori* and “acidophiles” could survive in harsh acidic environment.<sup>103</sup> So that this probe can be used to imaging strong acidity in bacteria. Moreover, in some eukaryotic cells, acidic pH affects organelles along the secretory and endocytic pathways.<sup>104,105</sup> Moreover, the fluorescence intensity of probe 6 is reversible between pH 1 and pH 7, which allows it to monitor a system with a shifty pH value and report the real time acidity. The probe is reversible, great selective and quickly responsive. We believe it will be beneficial to study in chemical and biological systems.

Xiao-Fan Zhang developed a coumarin-rhodamine probe 18 (Fig. 41) as a ratio metric pH probe in 2017.<sup>49</sup> When the probe interacted with  $\text{H}^+$ , the coumarin release decreased at 477 nm and the rhodamine release increased at 582 nm. The fluorescence intensity ratio responded linearly to minor pH changes in the range of 4.20–6.00. The probe showed high selectivity among different amino acids, metal cations and the ATP. Moreover, it has been successfully applied in fluorescence



18

Fig. 41 The structure of compound 18.



imaging in HeLa cells and the results indicated that the probe could selectively stain lysosome with low cytotoxicity and excellent photostability. We also applied **18** to monitor intracellular pH variations induced by dexamethasone. Therefore, **18** could act as a practical tool for the detection of pH in weakly acidic conditions and provide essential information in medicinal analysis and real biological systems.

### 4.3 Application in the detection of reactive O/S

**4.3.1 Fluorescence detection of reactive oxygen.** Reactive oxygen species (ROS) are involved in a variety of pathological diseases, played a significant role in keeping body health.<sup>106</sup> Hydroxyl radicals, is one of the most important ROS, and it can damage DNA, proteins, or membrane lipids and cause many diseases such as inflammations, embryo teratogenesis, herbicide effects, cell death, and killing of micro-organisms in pathogen-defence reactions.<sup>107</sup> Thus, developed new methods for detecting hydroxyl radicals in living cells have great meanings.

Lin Yuan *et al.* synthesized a new probe **56** (Fig. 42) which are really stable against auto-oxidation. The probe **56** as the first probe to achieve ratio metric fluorescent imaging of intracellular hydroxyl radicals. When interacting with hydroxyl radicals, the fluorescence intensity ratio of probe **56** at 495 and 651 nm ( $I_{651}/I_{495}$ ) increased significantly.<sup>108</sup>

Ji-Ting Hou *et al.* firstly designed a ratio-metric fluorescent probe **57** (Fig. 43) for  $\text{ClO}^-$  in 2015, which can sense  $\text{ClO}^-$  quickly and sensitively.<sup>109</sup> The probe reacted to  $\text{ClO}^-$  under alkaline conditions, and a new emission appeared at 580 nm.

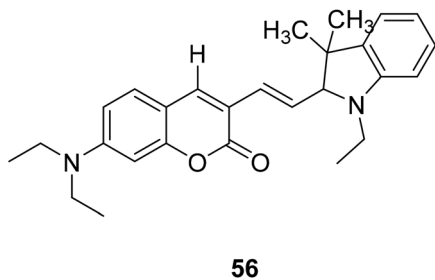


Fig. 42 The structure of compound **56**.

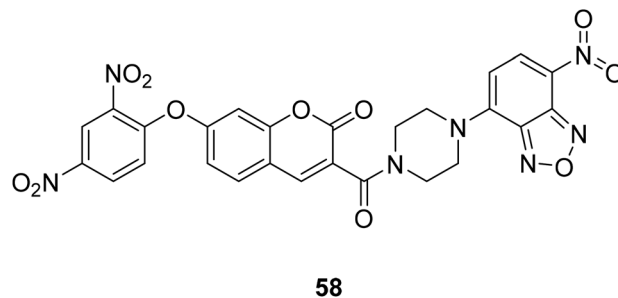


Fig. 44 The structure of compound **58**.

The emission intensity increased with the increase of hypochlorite dose, and the fluorescence intensity decreased at 470 nm. More importantly, **57** is the first mitochondria-targeted ratio-metric fluorescent probe to image exogenous and endogenous  $\text{ClO}^-$ .  $\text{ClO}^-$  produced by mitochondria has been linked to cancer. Therefore, a quantitative detection, especially *in situ* detection, of basal  $\text{ClO}^-$  in cancer cells is of significant interest.

**4.3.2 Fluorescence detection of active sulfur  $\text{H}_2\text{S}$ .** *In vivo*,  $\text{H}_2\text{S}$  is produced in many organs and tissues, catalysed by enzymes.<sup>110</sup> Hydrogen sulphide ( $\text{H}_2\text{S}$ ), as an endogenous gas compound, is involved in regulating a variety of physiological processes to maintain the health of the body. These physiological processes include regulation of inflammatory parts in the body,<sup>111</sup> relaxation of vasodilation, protection of vascular system,<sup>112</sup> influence insulin signal transmission,<sup>113</sup> intervention of nerve signal transmission,<sup>114</sup> anti-oxidation, and inhibit apoptosis of some cells in the body.  $\text{H}_2\text{S}$  can also inhibit leukocyte adherence in mesenteric microcirculation during vascular inflammation in rats, suggesting  $\text{H}_2\text{S}$  is a potent anti-inflammatory molecule. The concentration of  $\text{H}_2\text{S}$  was changed depend on physiological and pathological states.<sup>115</sup>

Zhang Changyu *et al.* designed a fluorescent probe **58** (Fig. 44) that interacts with  $\text{H}_2\text{S}$  in 2015.<sup>44</sup> It is reported that the probe has a large switching fluorescence response and can be used for biological imaging of endogenous  $\text{H}_2\text{S}$  in living cells. The probe interacted with  $\text{H}_2\text{S}$  and showed fluorescence quenching.

Bi-feng Chen and his team synthesized a coumarin fluorescent chemical probe **59** (Fig. 45) that detects  $\text{H}_2\text{S}$  in fetal bovine serum and degassed PBS buffer, a method with high selectivity

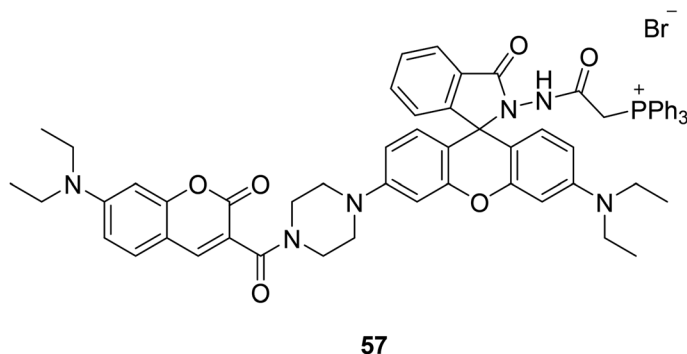
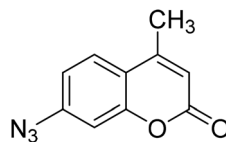


Fig. 43 The structure of compound **57**.



59

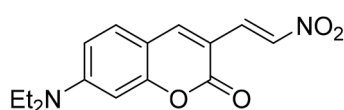
Fig. 45 The structure of compound 59.

and sensitivity in 2013.<sup>116</sup> The probe interacts with H<sub>2</sub>S to increase fluorescence. The probe can achieve *in situ* display of H<sub>2</sub>S in normal and AS rat heart tissues, and can also be used to screen agonists or antagonists of H<sub>2</sub>S synthase and tissue imaging. Therefore, this probe plays an important role in detecting H<sub>2</sub>S and maintaining body health.

Ming-Yu Wu *et al.* synthesized a colorimetric fluorescent probe **60** (Fig. 46) in 2012.<sup>117</sup> The probe can reduce nitro compounds to amines in the presence of H<sub>2</sub>S, so that it could be used to detect H<sub>2</sub>S. The probe interacts with H<sub>2</sub>S and generates a large emission displacement. The fluorescence probe provides a good method for the detection of hydrogen sulfide in the process of metabolism due to its fast response, high sensitivity and strong fluorescence ratio.

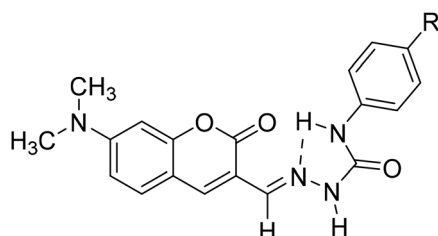
#### 4.4 Microenvironment polarity detection applications

Marek Cigán and his groups investigated four new efficient fluorescent “turn-on” probes **61**, **62**, **63**, **64** (Fig. 47) to sensing water in 2016.<sup>118</sup> All this coumarin fluorescence probes can response to low-level water content in polar aprotic solvents



60

Fig. 46 The structure of compound 60.

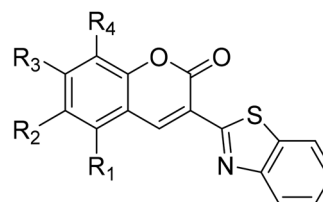


R=CN	<b>61</b>
=CF <sub>3</sub>	<b>62</b>
=F	<b>63</b>
=OCH <sub>3</sub>	<b>64</b>

Fig. 47 The structure of compound 61–64.

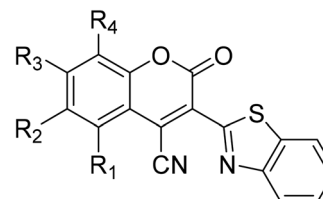
rapidly and reversibly, and the detection limits are amongst the lowest, even can compete in sensitivity with chemo dosimeters. Owing to that optical sensors for water sensing are flexibility, and it is possible to achieve remote monitoring, so that the probes for water sensing can be used in food processing, chemical reagents pharmaceutical manufacturing, and biomedical or environmental and the like. The specific performance is that when the probe meets with water in the polar aprotic solvents, we can see orange-yellow colour change and simultaneous fluorescence increase.

Giovanni Signore *et al.* synthesized coumarin fluorescence probes (**65a–d**, **66e–f**) (Fig. 48) which can be detected only in the most lipophilic environments of the cell in 2010.<sup>119</sup> The probe can be used as remarkable tools for studying subtle biochemical processes in the cellular environment when properly combined with biomolecules. Intracellular protein activity determines



65a-d

- a: R<sub>1</sub>=R<sub>4</sub>=H, R<sub>2</sub>=R<sub>3</sub>=OMe  
 b: R<sub>1</sub>=R<sub>2</sub>=H, R<sub>3</sub>=R<sub>4</sub>=OMe  
 c: R<sub>1</sub>=R<sub>2</sub>=H, R<sub>3</sub>=R<sub>4</sub>=-OCH<sub>2</sub>CH(COOEt)-O-  
 d: R<sub>1</sub>, R<sub>2</sub>=fused phenyl ring, R<sub>3</sub>=R<sub>4</sub>=H



66e-g

- e: R<sub>1</sub>=R<sub>4</sub>=H, R<sub>2</sub>=R<sub>3</sub>=OMe  
 f: R<sub>1</sub>=R<sub>2</sub>=H, R<sub>3</sub>=R<sub>4</sub>=OMe  
 g: R<sub>1</sub>=R<sub>2</sub>=H, R<sub>3</sub>=R<sub>4</sub>=-OCH<sub>2</sub>CH(COOEt)-O-

Fig. 48 The structure of compound 65a–d, 66e–g.



cellular behaviour, and the use of fluorescent probes and high-resolution imaging makes it possible to detect protein activity in the cellular environment. However, testing the activity of proteins in their completely natural state is not intrinsically feasible, and this problem can be solved by using a molecule that penetrates cells to selectively bind to a target protein in a certain state. These fluorescent molecules are extremely sensitive to environmental polarity and have good luminance in cells, which can be detected. It can be used as an indicator of environmental polarity change to reflect the biochemical process in cells. For example, coumarin without conjugate cyanide can be used as a fluorescent probe to detect the polarity of the environment. There is no fluorescence in water, but when the polarity of environment decreases, it shows strong fluorescence. Coumarin binds to protein and the same is true.

## 5. Conclusions

This review has highlighted the various aspects of coumarin fluorescent probes, including their chemical synthesis and application. Coumarin derivatives have good applications as fluorescent probes in many fields, such as detecting metal ions, environmental polarity, some disease-related active small molecules *in vivo*, etc. Ji Yun Ting *et al.* found a new coumarin-derived fluorescent probe **43**, which binds to Cu<sup>2+</sup> ions and shows obvious fluorescence quenching within the pH range of 5–9. It has been applied in living cells and the field of environmental food safety. Coumarin fluorescent probes are widely used in pharmaceutical chemistry. This paper reviews the synthesis of coumarin fluorescent probes based on different mechanisms and their applications in biochemical field. The detection of some active oxygen sulfur compounds by coumarin fluorescent probes provides great help for the diagnosis and treatment of cancer, and the monitoring of some heavy metal ions provides help for environmental protection. In the synthetic method, the fluorescent probes partially synthesized in the past ten years are summarized based on the position of the modified substituents on the coumarin mother nucleus.

Although the synthesis of coumarin fluorescent probes has made great progress, the structural optimization and modification still need to be further studied, and the application of coumarin probes also needs further exploration. At present, fluorescent probes can cause damage to some tumor cells, but there are few studies on their damage to normal cells. In the future, further studies on the damage of coumarin fluorescent probes to normal cells are needed to continuously reduce their harmful damage. The sensitivity of fluorescent probes needs to be improved. NIR fluorescence imaging has the advantages of deep tissue penetration, low background fluorescence interference and minimal light damage of biological samples, which has attracted people's attention. Therefore, further research is needed to improve the fluorescent probe to near-infrared. Now, to design ratiometric probes with the mechanism of fluorescence resonance energy transfer (FRET) system has many advantages. It can reduce fluorescence detection error and self-quenching.<sup>120–122</sup> It is still a problem worth studying to fabricate fluorescent chemo-sensors based on the FRET system. It is

hoped that the ideas and examples cited in this review article will further stimulate and optimize the full potential of coumarin-based fluorescent probes, improve design selectivity, realize more simple and efficient applications in more fields, and help in the treatment of diseases.

## Conflicts of interest

The authors declare that this article content has no conflict of interest.

## Acknowledgements

The authors are grateful to the Shandong Provincial Academy of Medical Sciences for the scientific research project (2019–18), and the Shandong Natural Science Foundation [ZR2018LH021].

## Notes and references

- 1 X. Q. Li, J. P. Gu, Z. Zhou, L. F. Ma, Y. H. Zheng, Y. P. Tang, J. W. Gao and Q. M. Wang, *Chem. Eng. J.*, 2019, **358**, 67–73.
- 2 P. P. Deshmukh, A. Navalkar, S. K. Maji and S. T. Manjare, *Sens. Actuators, B*, 2018, **281**, 8–13.
- 3 X. H. Cheng, H. Z. Jia, T. Long, J. Feng, J. G. Qin and Z. Li, *Chem. Commun.*, 2011, **47**(43), 11978–11980.
- 4 N. T. Wu, Y. P. Tang, M. Zeng, J. W. Gao, X. B. Lu and Y. H. Zheng, *J. Lumin.*, 2018, **202**, 502–507.
- 5 D. Lu, Y. P. Tang and Y. H. Zheng, *J. Fluoresc.*, 2018, **28**(6), 1269–1273.
- 6 X. Q. Li, Z. Zhou, C. C. Zhang, Y. H. Zheng, J. W. Gao and Q. M. Wang, *Inorg. Chem.*, 2018, **57**(15), 8866–8873.
- 7 N. Soh, Y. Katayama and M. Maeda, *Analyst*, 2001, **126**(5), 564–566.
- 8 K. Tanaka, T. Miura, N. Umezawa, Y. Urano, K. Kikuchi, T. Higuchi and T. Nagano, *J. Am. Chem. Soc.*, 2001, **123**(11), 2530–2536.
- 9 R. Su, J. W. Gao, S. R. Deng, R. H. Zhang and Y. H. Zheng, *J. Sol-Gel Sci. Technol.*, 2016, **78**(3), 606–612.
- 10 C. F. Yu, Z. Y. Zhang, M. Z. Fu, J. W. Gao and Y. H. Zheng, *J. Electron. Mater.*, 2017, **46**(10), 5895–5900.
- 11 S. L. Gui, Y. Y. Huang, F. Hu, Y. L. Jin, G. X. Zhang, L. S. Yan, D. Q. Zhang and R. Zhao, *Anal. Chem.*, 2015, **87**(3), 1470–1474.
- 12 Z. Zhou, C. C. Zhang, Y. H. Zheng and Q. M. Wang, *Dyes Pigm.*, 2018, **150**, 151–157.
- 13 B. L. Sui, S. M. Tang, T. H. Liu, B. S. Kim and K. D. Belfield, *ACS Appl. Mater. Interfaces*, 2014, **6**(21), 18408–18412.
- 14 V. S. Lin, W. Chen, M. Xian and C. J. Chang, *Chem. Soc. Rev.*, 2015, **44**(14), 4596–4618.
- 15 Y. H. Tang, D. Lee, J. L. Wang, G. H. Li, J. H. Yu, W. Y. Lin and J. Yoon, *Chem. Soc. Rev.*, 2015, **44**(15), 5003–5015.
- 16 X. Q. Li, Z. Zhou, Y. P. Tang, C. C. Zhang, Y. H. Zheng, J. W. Gao and Q. M. Wang, *Sens. Actuators, B*, 2018, **276**, 95–100.
- 17 J. P. Gu, X. Q. Li, Z. Zhou, R. S. Liao, J. W. Gao, Y. P. Tang and Q. M. Wang, *Chem. Eng. J.*, 2019, **368**, 157–164.





- 18 F. Borges, F. Roleira, N. Milhazes, L. Santana and E. Uriarte, *Curr. Med. Chem.*, 2005, **12**(30), 887–916.
- 19 M. F. M. R. Borges, F. M. F. Roleira, N. J. D. S. P. Milhazes, E. U. Villares and L. S. Penin, *Front. Chem.*, 2009, **4**(8), 23–85.
- 20 G. B. Bubols, D. R. Vianna, A. Medina-Reimon, G. VonPoser, R. M. Lamuela-Raventos, V. L. Eifler-Lima and S. C. Garcia, *Mini-Rev. Med. Chem.*, 2013, **13**(3), 318–322.
- 21 S. E. Bariamis, M. Marin, C. M. Athanassopoulos, C. Kontogiorgis, Z. Tsimal, D. Papaioannou, G. Sindona, G. Romeo, K. Avgoustakis and D. Hadjipavlou-Litina, *Eur. J. Med. Chem.*, 2013, **60**, 155–169.
- 22 M. J. Matos, L. Santana, E. Uriarte, G. Delogu, M. Corda, M. B. Fadda, B. Era and A. Fais, *Bioorg. Med. Chem. Lett.*, 2011, **21**(11), 3342–3348.
- 23 H. M. Revankar, S. N. A. Bukhari, G. B. Kumar and H. L. Qin, *Bioorg. Chem.*, 2017, **71**, 146–159.
- 24 Y. Jeong and J. Yoon, *Inorg. Chim. Acta*, 2012, **381**, 2–14.
- 25 C. J. Wu, J. B. Wang, J. J. Shen, C. Bi and H. W. Zhou, *Sens. Actuators, B*, 2017, **243**, 678–683.
- 26 H. Kobayashi, M. Ogawa, R. Alford, P. L. Choyke and Y. Urano, *Chem. Rev.*, 2010, **110**(5), 2620–2640.
- 27 E. Ruoslahti, *Annu. Rev. Cell Dev. Biol.*, 1996, **12**, 697–715.
- 28 H. Y. Song, M. H. Ngai, Z. Y. Song, P. A. MacAry, J. Hobley and M. J. Lear, *Org. Biomol. Chem.*, 2009, **7**(17), 3400–3406.
- 29 I. Wallace, M. Davis, L. Munro, V. J. Catalano, P. J. Cragg, M. T. Huggins and K. J. Wallace, *Org. Lett.*, 2012, **14**(11), 2686–2689.
- 30 Z. R. Grabowski, K. Rotkiewicz and W. Rettig, *Chem. Rev.*, 2003, **103**(10), 3899–4032.
- 31 R. R. Hu, E. Lager, A. Aguilar, J. C. Liu, W. Jacky, H. H.-Y. Sung, L. D. Williams, Y. C. Zhong, K. S. Wong and B. Z. Tang, *J. Phys. Chem. C*, 2009, **113**(36), 15845–15853.
- 32 H. Sahoo, *J. Photochem. Photobiol., C*, 2011, **12**(1), 20–30.
- 33 A. P. Silva, T. S. Moody and G. D. Wright, *Analyst*, 2009, **134**(12), 2385–2393.
- 34 F. A. Khan, K. Parasuraman and K. K. Sadhu, *Chem. Commun.*, 2009, **134**(17), 2399–2401.
- 35 E. Tamanini, A. Katewa, L. M. Sedger, M. H. Todd and M. Watkinson, *Inorg. Chem.*, 2009, **48**(1), 319–324.
- 36 N. Boens, V. Leen and W. Dehaen, *Chem. Soc. Rev.*, 2012, **41**(24), 1130–1172.
- 37 Y. H. Fu and N. Finney, *RSC Adv.*, 2018, **8**(51), 29051–29061.
- 38 S. Voutsadaki, G. K. Tsikalas, E. Klontzas and G. E. Froudakis, *Chem. Commun.*, 2010, **46**(19), 3292–3294.
- 39 G. Shanker, L. A. Mutkus, S. J. Walker and M. Aschner, *Mol. Brain Res.*, 2002, **106**(1–2), 1–11.
- 40 Y. Xu, Z. Jiang, Y. Xiao, F. Z. Bi, J. Y. Miao and B. X. Zhao, *Anal. Chim. Acta*, 2014, **820**, 146–151.
- 41 L. Yi, H. Y. Li, L. Sun, L. L. Liu, C. H. Zhang and Z. Xi, *Angew. Chem., Int. Ed.*, 2009, **48**(22), 4034–4037.
- 42 K. S. Lee, T. K. Kim, J. H. Lee, H. J. Kim and J. I. Hong, *Chem. Commun.*, 2008, **14**(46), 6173–6175.
- 43 M. H. Lee, J. S. Kim and J. L. Sessler, *Chem. Soc. Rev.*, 2015, **44**(13), 4185–4191.
- 44 C. Y. Zhang, L. Wei, C. Wei, J. Zhang, R. Wang, Z. Xi and L. Yi, *Chem. Commun.*, 2015, **51**(35), 7505–7508.
- 45 J. Li, C. F. Zhang, Z. Z. Ming, W. C. Yang and G. F. Yang, *RSC Adv.*, 2013, **3**(48), 26059–26065.
- 46 A. E. Albers, V. S. Okreglak and C. J. Chang, *J. Am. Chem. Soc.*, 2006, **128**(30), 9640–9641.
- 47 C. Y. Zhang, L. Wei, C. Wei, J. Zhang, R. Y. Wang, Z. Xi and L. Yi, *Chem. Commun.*, 2015, **51**(52), 10510–10513.
- 48 M. Tasior, D. Kim, S. Singha, M. Krzeszewski, K. H. Ahn and D. T. Gryko, *J. Mater. Chem. C*, 2015, **3**(7), 1421–1446.
- 49 X. F. Zhang, T. Zhang, S. L. Shen, J. Y. Miao and B. X. Zhao, *RSC Adv.*, 2013, **5**(61), 49115–49121.
- 50 D. En, Y. Guo, B. T. Chen, B. Dong and M. J. Peng, *RSC Adv.*, 2014, **4**(1), 248–253.
- 51 Y. C. Chen, C. M. Clouthier, K. Tsao, M. Strmiskova, H. Lachance and J. W. Keillor, *Angew. Chem., Int. Ed.*, 2014, **53**(50), 1–5.
- 52 Q. H. You, A. W. M. Lee, W. H. Chan, X. M. Zhu and K. C. F. Leung, *Chem. Commun.*, 2014, **50**(47), 6207–6210.
- 53 K. B. Zheng, W. Y. Lin, L. Tan, H. Chen and H. J. Cui, *Chem. Sci.*, 2014, **5**(9), 3439–3448.
- 54 X. W. Cao, W. Y. Lin and Q. X. Yu, *J. Org. Chem.*, 2011, **76**(18), 7423–7430.
- 55 D. Jung, S. Maiti, J. H. Lee, J. H. Lee and J. S. Kim, *Chem. Commun.*, 2014, **50**(23), 3044–3047.
- 56 M. H. Yan, T. R. Li and Z. Y. Yang, *Inorg. Chem. Commun.*, 2011, **14**, 463–465.
- 57 X. H. Fang, J. J. Li, J. Perlette, W. H. Tan and K. M. Wang, *Anal. Chem.*, 2000, **72**(23), 747A–753A.
- 58 A. Bekhradnia, E. Domehri and M. Khosravi, *Spectrochim. Acta, Part A*, 2016, **152**(5), 18–22.
- 59 D. Maity, D. Karthigeyan, T. K. Kundu and T. Govindaraju, *Sens. Actuators, B*, 2013, **176**, 831–837.
- 60 J. T. Yeh, W. C. Chen, S. R. Liu and S. P. Wu, *New J. Chem.*, 2014, **38**(9), 4434–4439.
- 61 H. S. Jung, P. S. Kwon, J. W. Lee, J. I. Kim, C. S. Hong, J. W. Kim, S. H. Yan, J. Y. Lee, J. H. Lee, T. Joo and J. S. Kim, *J. Am. Chem. Soc.*, 2009, **131**(5), 2008–2012.
- 62 A. Bekhradnia, E. Domehri and M. Khosravi, *Spectrochim. Acta, Part A*, 2016, **152**, 18–22.
- 63 W. Y. Lin, L. Yuan, W. Tan, J. B. Feng and L. L. Long, *Chem.–Eur. J.*, 2009, **15**, 1030–1035.
- 64 A. Bekhradnia, E. Domehri and M. Khosravi, *Spectrochim. Acta, Part A*, 2016, **152**, 18–22.
- 65 X. Chen, S. W. Nam, G. H. Kim, N. Song, Y. Jeong, I. Shin, S. K. Kim, J. Kim, S. Park and J. Yoon, *Chem. Commun.*, 2010, **46**(47), 8953–8955.
- 66 J. T. Hou, K. Li, K. K. Yu, M. Y. Wu and X. Q. Yu, *Org. Biomol. Chem.*, 2013, **11**(5), 717–720.
- 67 J. S. Lee, M. S. Han and C. A. Mirkin, *Angew. Chem., Int. Ed.*, 2007, **46**(22), 4093–4096.
- 68 E. M. Nolan and S. J. Lippard, *Chem. Rev.*, 2008, **108**(9), 3443–3480.
- 69 I. Onyido, A. R. Norris and E. Buncel, *Chem. Rev.*, 2004, **104**(12), 5911–5929.
- 70 X. Q. Chen, X. Z. Tian, I. Shin and J. Yoon, *Chem. Soc. Rev.*, 2011, **40**(9), 4783–4804.



- 71 J. W. Hu, Z. J. Hu, S. Liu, Q. Zhang, H. W. Gao and K. Uvdal, *Sens. Actuators, B*, 2016, **230**, 639–644.
- 72 J. Ding, H. Li, C. Wang, J. Yang, Y. Xie, Q. Peng, Q. Li and Z. Li, *ACS Appl. Mater. Interfaces*, 2015, **7**(21), 11369–11376.
- 73 Y. Y. Yan, Y. H. Zhang and H. Xu, *ChemPlusChem*, 2013, **78**(7), 628–631.
- 74 M. Hong, S. Lu, F. Lv and D. Xu, *Dyes Pigm.*, 2016, **127**, 94–99.
- 75 S. L. Kao and S. P. Wu, *Sens. Actuators, B*, 2015, **212**, 382–388.
- 76 S. Erdemir, O. Kocyigit and S. Karakurt, *Sens. Actuators, B*, 2015, **220**, 381–388.
- 77 Q. Zou, L. Zou and W. J. Wu, *J. Mater. Chem.*, 2011, **21**(38), 14441–14447.
- 78 Q. J. Ma, X. B. Zhang, X. H. Zhao, Z. Jin, G. J. Mao, G. L. Shen and R. Q. Yu, *Anal. Chim. Acta*, 2010, **663**(1), 85–90.
- 79 W. M. Xuan, C. Chen, Y. T. Cao, W. H. He, W. Jiang, K. J. Liu and W. Wang, *Chem. Commun.*, 2012, **48**(58), 7292–7294.
- 80 F. J. Huo, Y. Q. Sun, J. Su, Y. T. Yang, C. X. Yin and J. B. Chao, *Org. Lett.*, 2010, **12**(21), 4756–4759.
- 81 R. Bogoroch and L. F. Belanger, *Anat. Rec.*, 1975, **183**(3), 437–447.
- 82 W. Jahnen-Dechent and M. Ketteler, *Magnesium, Basics, Clin. Kidney J.*, 2012, **5**(suppl 1), i3–i14.
- 83 R. Swaminathan, *Clin. Biochem. Rev.*, 2003, **24**(2), 47–66.
- 84 V. K. Gupta, M. Naveen and L. K. Kumawat, *Sens. Actuators, B*, 2015, **207**, 216–223.
- 85 D. Ray and P. K. Bharadwaj, *Inorg. Chem.*, 2008, **47**, 2252–2254.
- 86 H. J. Yin, B. C. Zhang, H. Z. Yu, L. Zhu, Y. Feng, M. Z. Zhu, Q. X. Guo and X. M. Meng, *J. Org. Chem.*, 2015, **80**(9), 4306–4312.
- 87 T. Fujii, Y. Shindo, K. Hotta, D. Citterio, S. Nishiyama, K. Suzuki and K. Oka, *J. Am. Chem. Soc.*, 2014, **136**(6), 2374–2381.
- 88 K. Li and A. J. Tong, *Sens. Actuators, B*, 2013, **184**, 248–253.
- 89 R. McRae, P. Bagchi, S. Sumalekshmy and C. J. Fahrni, *Chem. Rev.*, 2009, **109**(10), 4780–4827.
- 90 L. J. Tang, M. J. Cai, P. Zhou, J. Zhao, K. L. Zhong, S. H. Hou and Y. J. Bian, *RSC Adv.*, 2013, **3**(37), 16802–16809.
- 91 J. C. Qin, L. Fan and Z. Y. Yang, *Sens. Actuators, B*, 2016, **228**, 156–161.
- 92 W. Zhang, P. Li, F. Yang, X. Hu, C. Sun, W. Zhang, D. Chen and B. Tang, *J. Am. Chem. Soc.*, 2013, **135**(40), 14956–14959.
- 93 Q. Q. Wu, Z. F. Xiao, X. J. Du and Q. H. Song, *Chem.-Asian J.*, 2013, **8**(11), 2564–2568.
- 94 L. Li, J. Y. Ge, H. Wu, Q. H. Xu and S. Q. Yao, *J. Am. Chem. Soc.*, 2012, **134**(29), 12157–12167.
- 95 S. Mizukami, S. Okada, S. Kimura and K. Kikuchi, *Inorg. Chem.*, 2009, **48**(16), 7630–7638.
- 96 D. Perez-Sala, D. Collado-Escobar and F. Mollinedo, *J. Biol. Chem.*, 1995, **270**(11), 6235–6242.
- 97 B. C. Dickinson, D. Srikun and C. J. Chang, *Curr. Opin. Chem. Biol.*, 2010, **14**(1), 50–56.
- 98 T. Ueno and T. Nagano, *Nat. Methods*, 2011, **8**(8), 642–645.
- 99 Z. G. Yang, J. F. Cao, Y. X. He, J. H. Yang, T. Kim, X. J. Peng and J. S. Kim, *Chem. Soc. Rev.*, 2014, **43**(13), 4563–4601.
- 100 B. C. Dickinson and C. J. Chang, *J. Am. Chem. Soc.*, 2008, **130**(30), 9638–9639.
- 101 E. Tomat, E. M. Nolan, J. Jaworski and S. J. Lippard, *J. Am. Chem. Soc.*, 2008, **130**(47), 15776–15777.
- 102 S. S. Zhu, W. Y. Lin and Y. Lin, *Dyes Pigm.*, 2013, **99**(2), 465–471.
- 103 H. L. Li, H. Guan, X. R. Duan, J. Hu, G. R. Wang and Q. Wang, *Org. Biomol. Chem.*, 2013, **11**(11), 1805–1809.
- 104 T. A. Krulwich, G. Sachs and E. Padan, *Nat. Rev. Microbiol.*, 2011, **9**(5), 330–343.
- 105 G. Loving and B. Imperiali, *J. Am. Chem. Soc.*, 2008, **130**(41), 13630–13638.
- 106 C. T. Chu, D. J. Levinthal, S. M. Kulich, E. M. Chalovich and D. B. DeFranco, *Eur. J. Biochem.*, 2004, **271**, 2060–2066.
- 107 C. J. Stephanson, A. M. Stephanson and G. P. Flanagan, *J. Med. Food*, 2003, **6**(3), 249–253.
- 108 L. Yuan, W. Y. Lin and J. Song, *Chem. Commun.*, 2010, **46**(42), 7930–7932.
- 109 J. T. Hou, K. Lin, J. Yang, K. K. Yu, Y. X. Liao, Y. Z. Ran, Y. H. Liu, X. D. Zhou and X. Q. Yu, *Chem. Commun.*, 2015, **51**(31), 6781–6784.
- 110 B. L. Predmore, D. J. Lefer and G. Gojon, *Antioxid. Redox Signaling*, 2012, **17**(1), 119–140.
- 111 L. Li, M. Bhatia and P. K. Moore, *Curr. Opin. Pharmacol.*, 2006, **6**(2), 125–129.
- 112 G. D. Yang, L. Y. Wu, B. Jiang, W. Yang, J. S. Qi, K. Cao, Q. H. Meng, A. K. Mustafa, W. T. Mu, S. M. Zhang, S. H. Snyder and R. Wang, *Science*, 2008, **322**(5901), 587–590.
- 113 L. Wu, W. Yang, X. Jia, G. Yang, D. Duridanova, K. Cao and R. Wang, *Lab. Invest.*, 2008, **89**(1), 59–67.
- 114 L. F. Hu, M. Lu, Z. Y. Wu, P. T. Wong and J. S. Bian, *Mol. Pharmacol.*, 2009, **75**(1), 27–34.
- 115 W. H. Li, W. Sun, X. Q. Yu, L. P. Du and M. Y. Li, *J. Fluoresc.*, 2013, **23**(1), 181–186.
- 116 B. F. Chen, W. Li, C. Lv, M. M. Zhao, H. W. Jin, H. F. Jin, J. B. Du, L. R. Zhang and X. J. Tang, *Analyst*, 2013, **138**(3), 946–951.
- 117 M. Y. Wu, K. Li, J. T. Hou, Z. Huang and X. Q. Yu, *Org. Biomol. Chem.*, 2012, **10**(41), 8342–8347.
- 118 M. Cigán, J. Gašpar, K. Gáplovská and J. Holeksiova, *New J. Chem.*, 2016, **40**(10), 8946–8953.
- 119 G. Signore, R. Nifosi, L. Albertazzi, B. Storti and R. Bizzarri, *J. Am. Chem. Soc.*, 2010, **132**(4), 1276–1288.
- 120 D. Udhayakumari, S. Naha and S. Velmathi, *Anal. Methods*, 2017, **9**(4), 552–578.
- 121 N. I. Georgiev, A. M. Asiri, A. H. Qusti, K. A. Alamry and V. B. Bojinov, *Dyes Pigm.*, 2014, **102**, 35–45.
- 122 S. L. Casciato, H. M. Liljestrand and J. A. Holcombe, *Anal. Chim. Acta.*, 2014, **813**, 77–82.

